Biomaterials Science

Liposomal MRI probes containing encapsulated or amphiphilic Fe(III) coordination complexes

Journal:	*Biomaterials Science*
Manuscript ID	BM-ART-01-2023-000029.R2
Article Type:	Paper
Date Submitted by the Author:	21-Jun-2023
Complete List of Authors:	Chowdhury, Md Saiful; University at Buffalo, SUNY, chemistry Kras, Elizabeth; University at Buffalo, SUNY, chemistry Turowski, Steven; Roswell Park Comprehensive Cancer Center Spernyak, Joseph; Roswell Park Cancer Institute, Department of Cell Stress Biology Morrow, Janet; University at Buffalo, SUNY, chemistry

Liposomal MRI probes containing encapsulated or amphiphilic Fe(III) coordination complexes

*Md Saiful I. Chowdhury,[1] Elizabeth A. Kras,[1] Steven G. Turowski,[2] Joseph A. Spernyak[2] and Janet R. Morrow[1]**

[1] Department of Chemistry, University at Buffalo, The State University of New York Amherst, NY 14260, United States

[2] Department of Cell Stress Biology, Roswell Park Comprehensive Cancer Center, Buffalo, New York 14263, United States

* to whom correspondence should be addressed at: jmorrow@buffalo.edu

Abstract

Liposomes containing high-spin Fe(III) coordination complexes were prepared towards the production of T_1 MRI probes with improved relaxivity. The amphiphilic Fe(III) complexes were anchored into the liposome with two alkyl chains to give a coordination sphere containing mixed amide and hydroxypropyl pendant groups. The encapsulated complex contains a macrocyclic ligand with three phosphonate pendants, $[Fe(NOTP)]^{3-}$, which was chosen for its good aqueous solubility. Four types of MRI probes were prepared including those with intraliposomal Fe(III) complex (LipoA) alone, amphiphilic Fe(III) complex (LipoB), both intraliposomal and amphiphilic complex (LipoC) or micelles formed with amphiphilic complex. Water proton relaxivities r_1 and r_2 were measured and compared to a small molecule macrocyclic Fe(III) complex containing similar donor groups. Micelles of the amphiphilic Fe(III) complex had proton relaxivity values (r_1 = 2.6 $mM^{-1}s^{-1}$) that were four times higher than the small hydrophilic analog. Liposomes with amphiphilic Fe(III) complex (LipoB) have a per iron relaxivity of 2.6 $mM^{-1}s^{-1}$ at pH 7.2, 34 °C at 1.4 T whereas liposomes containing both amphiphilic and intraliposomal Fe(III) complexes (lipoC) have r_1 of 0.58 $mM^{-1}s^{-1}$ on a per iron basis consistent with quenching of the interior Fe(III) complex relaxivity. Liposomes containing only encapsulated $[Fe(NOTP)]^{3-}$ have a lowered r_1 of 0.65 $mM^{-1}s^{-1}$ per iron complex. Studies show that the biodistribution and clearance of the different types liposomal nanoparticles differ greatly. LipoB is a blood pool agent with a long circulation time whereas lipoC is cleared more

rapidly through both renal and hepatobiliary pathways. These clearance differences are consistent with lower stability of LipoC compared to LipoB.

Introduction

Paramagnetic liposomes have been studied extensively as contrast agents for the modulation of water proton relaxation in T_1 weighted magnetic resonance imaging (MRI).[1-3] Such liposomal agents amplify water proton relaxation by incorporation of tens of thousands of paramagnetic complexes, generally Gd(III)-based, per particle.[2, 4] This amplification serves to increase the contrast signal to noise produced by probes, facilitating their use in challenging applications in molecular imaging.[1, 5] For example, liposomal MRI probes with high relaxivity may be functionalized by attachment of recognition moieties such as oligopeptides, proteins, antibodies, and target-specific phospholipids. Such targeted liposomes have been used for molecular imaging including to image tumor endothelium with cyclic RGD peptides,[6] to target endothelial integrins that are overexpressed in tumors, and as tools for imaging angiogenesis.[7] Paramagnetic liposomes also serve as drug carriers that can be tracked for monitoring drug distribution and release for MRI guided drug delivery.[1]

Paramagnetic metal complexes incorporated into liposomes are most commonly Gd(III) complexes.[4, 8] Gd(III) containing liposomes have been studied as T_1 and T_2 agents as well as liposomal CEST agents.[9] While Gd(III)-based probes show promise in molecular imaging through the incorporation of targeting moieties or activatable ligands,[10] paramagnetic transition metal complexes bring another level of responsiveness to molecular imaging through their ability to change oxidation states, spin states and their unique solution chemistry.[11-13] Moreover transition metal complexes, especially those of high-spin Mn(II) and Fe(III) are of interest as alternatives for Gd(III) agents given that both metals are biocompatible and both have an electronic configuration that enables their development as T_1 agents.[11, 12, 14-16] Co(II) and Cu(II) have less favorable properties as T_1 agents,[17] and most studies of these metal ions feature applications as redox-responsive agents.[13, 18] Fe(III) agents in particular are of interest for further development in light of the body's ability to sequester, store and recycle iron.[19] While Mn(II) agents have been used in humans in early studies and improved versions are

under development,[20] studies of Fe(III) complexes as MRI contrast agents has lagged behind. Fe(III) complexes were investigated in early studies of MRI contrast agents,[21] but interest decreased as Gd(III) agents were developed. Interest in Fe(III)-based MRI probes has increased recently with several new reports highlighting the challenges of their development as coordination complexes[11, 12, 14, 15, 22, 23] and in nanostructures.[24]

Our laboratory focuses on the development of transition metal MRI probes, including CEST agents (Fe(II), Co(II) and Ni(II)),[13, 25] liposomal CEST agents[26] and relaxivity agents such as high-spin Fe(III) complexes.[12] The development of Fe(III) based agents has many challenges including overcoming low water solubility and lowered relaxivity[12, 27-29] and complicated solution chemistry.[30] Recently, we reported on an Fe(III)-based liposomal MRI probe that was studied in solution and in mice.[28] Our study featured macrocyclic complexes of Fe(III) containing hydroxypropyl pendants that are effective in promoting second-sphere water interactions. One Fe(III) complex had an amphiphilic tail and hydroxypropyl pendants and the encapsulated complexes contained only hydroxypropyl pendants. This study was one of the first reported liposomal agents containing Fe(III) coordination complexes. However, the encapsulated Fe(III) complexes used in this earlier study were cationic (Figure 1), and clear very slowly from mice with substantial kidney retention even after 4 hours.[28] Moreover, the amphiphilic complex was attached via a single alkyl chain by using a ring opening reaction to produce a mixture of stereoisomers, an undesirable characteristic for the study of MRI probes. An earlier study reported on liposomal Fe(III) agents of polyaminocarboxylate ligands that were unstable and aggregated in solution.[31] A more recent study featured an Fe(III) complex of succinyl-deferoxamine loaded into the interior of the liposome that was released by high intensity ultrasound heating of the tumor.[32] This study illustrated the propensity of liposomes to accumulate in tumors by extravasation through the leaky endothelial cell barrier. Such properties make liposomes ideal nanocarriers for imaging tumors and the delivery of anticancer drugs.[1, 33]

Paramagnetic complexes encapsulated in the interior of liposomes show reduced relaxivity compared to free paramagnetic metal ion complexes due to quenching of water proton relaxation by limited exchange of water across the bilayer.[34, 35] Incorporation of

amphiphilic agents into the bilayer is one approach to increase the relaxivity per particle due to direct interaction of the complex with the bulk water from the complexes on the exterior of the liposome.[34, 36] Here we present the first Fe(III) amphiphilic coordination complex with a two alkyl chain anchor connected by way of a synthetically versatile amide linkage and compare the relaxivity of the liposomal and analogous non-liposomal Fe(III) complex to assess the effect of incorporation into the liposome. In addition to the liposomes, micelles of this amphiphilic Fe(III) complex are prepared and compared as MRI probes. Micelles have the advantage of being simple nanoparticles of 10-50 nm with a core-shell architecture.

To further increase per particle relaxivity and to explore the effect of an encapsulated iron-based MRI probe on liposomal clearance, an anionic Fe(III) complex was loaded into the interior of liposomes with or without an amphiphilic Fe(III) complex in the bilayer. The anionic complex, $[Fe(NOTP)]^{3-}$ has slightly reduced relaxivity compared to the cationic complex, $[Fe(NOHP)]^{2+}$ studied previously, but has a different biodistribution and clearance pathway.[37] The new liposomal agents are studied for biodistribution in mice with CT26 colorectal cancer tumor models. The three types of liposomes show differences in biodistribution and clearance that may be useful for further development of agents that contain encapsulated probes. For example, studies here focus on stabilized trivalent iron complexes as cargo to track their biodistribution by MRI, but future applications with the encapsulation of responsive contrast agents in liposomes are of interest. Such dual-labeled liposomes may provide new types of MRI probes.

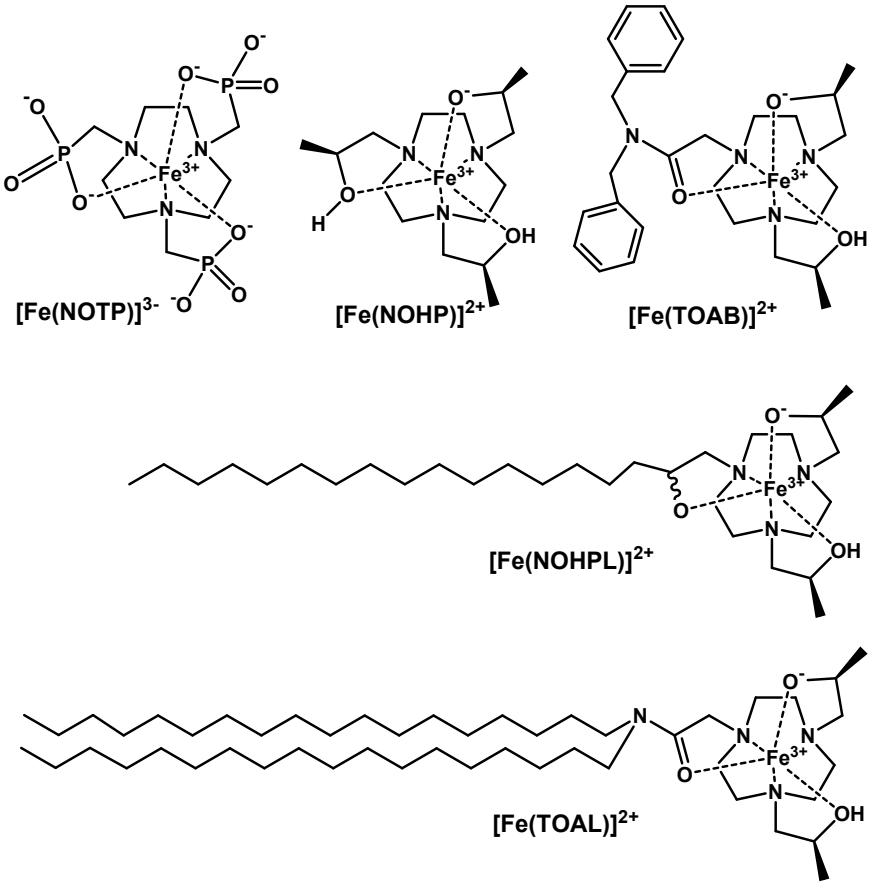

Figure 1. Iron(III) complexes discussed in this study with speciation shown at neutral pH.

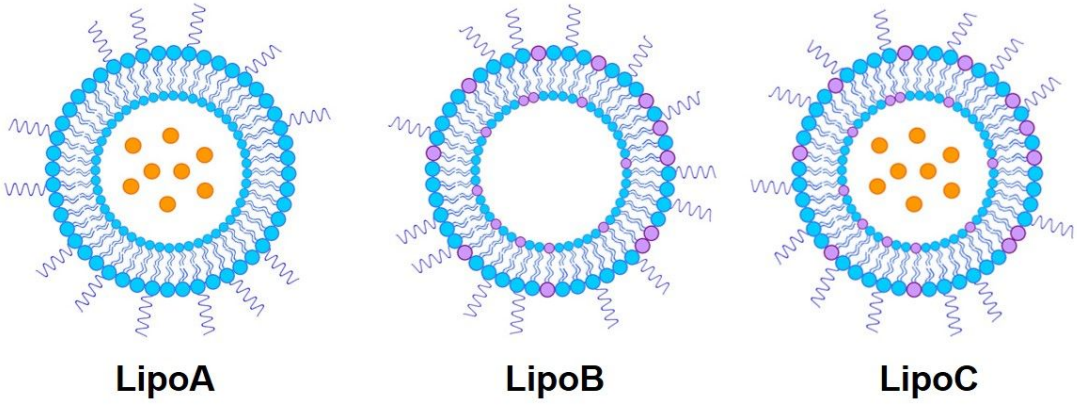

Figure 2. Pegylated liposome types studied here with a) $[Fe(NOTP)]^{3-}$ complex (orange spheres) incorporated into the liposomal lumen, b) $[Fe(TOAL)]^{2+}$ (purple spheres) incorporated into bilayer or c) $[Fe(NOTP)]^{3-}$ incorporated into lumen and $[Fe(TOAL)]^{2+}$ incorporated into bilayer.

2. Experimental and methods section

***2.1 Instrumentation*.** A Varian Inova 500 MHz NMR spectrometer (11.7 T) equipped with FTS Systems TC-84 Kinetics Air Jet Temperature Controller or a Bruker Neo 500 MHz spectrometer was used to collect ^{1}H NMR spectra. ^{13}C NMR spectra were acquired using a Varian Mercury 300 MHz, 400 MHz NMR spectrometer, or a Bruker Neo 500 MHz spectrometer. Proton relaxivity experiments were performed at 1.4 T (34 ^{o}C) on a Nananalysis NMR spectrometer, at 4.7 T, or on a Bruker preclinical MRI scanner or at 9.4 T, or on a Varian Inova 400 MHz NMR spectrometer at variable temperatures. All pH measurements were made by utilizing an Orion 8115BNUWP Ross Ultra Semi Micro pH electrode connected to a 702 SM Titrino pH. Thermo Fisher Linear Ion Trap (LTQ) LC/MS equipped with a Surveyor HPLC system was used to for mass spectrometry data of the complexes. Iron concentration was determined by using a Thermo X-Series 2 ICP-MS and UV-vis spectrometry as reported.[29, 38] A Zetasizer instrument from Malvern Panalytical Ltd. was used for DLS measurements of liposomal size and zeta potential.

2.1 Reagents. DPPC, DSPE-PEG2000, and cholesterol were purchased from Avanti Polar Inc. (Alabaster, Al, USA). (S)-(−)-Propylene oxide; N,N-dimethyl-2-chloro acetamide, N,N-dioctadecylamine were purchased from Sigma-Aldrich and 2-chloro acetyl chloride was purchased from Acros Organics in USA. N, N-Diisopropylethylamine (DIPEA) was purchased from BeanTown Chemical. Ferrous chloride tetrahydrate was purchased from Alfa Aesar and ferrous bromide anhydrous was purchased from ThermoFisher Scientific. The NOTP ligand and its iron complex, $Na_3[Fe(NOTP)]$ was prepared as reported.[37] 2-chloro-N,N-dibenzylacetamide was synthesized as previously reported by Bernier et al.[39] (2S,2'S)-1,1'-(1,4,7-triazonane-1,4-diyl)bis(propan-2-ol) (0.060 mmol) was prepared as reported.[27, 40]

2.2 Synthesis of ligands and complexes

2.2.1 Synthesis of N,N-distearoyl-2-chloro acetamide and TOALH ligand. In a 250 mL round-bottom flask, 1 mmol of N,N-dioctadecylamine was dissolved in 150 ml acetonitrile : dichloromethane (70:30) mixture at 55 °C and 4-5 equivalent of dipotassium phosphate (K_2HPO_4) was added to this solution. 1.05 mmol (1.05 eq) of 2-chloro acetyl chloride was diluted in 25 ml

dichloromethane at room temperature and slowly added to the dissolved N,N-dioctadecylamine solution over an hour at 55-60 °C. The solution was stirred at 60 °C for a day. Then the solution was filtered and the solid was washed with chloroform. The filtrate was dried under reduced pressure and a white solid was recovered as residue. It was partitioned in water and chloroform. The chloroform layer was dried with anhydrous sodium sulfate, filtered and removed under reduced pressure. This yielded N,N-distearoyl-2-chloro-acetamide as white solid (98-99%). The product was characterized using ^{1}H NMR and ^{13}C NMR (Figure S1a and S2a). **^{1}H NMR:** (400 MHz, $CDCl_3$): δ 4.04 (2H, ClC**H_2**-$CONR_2$), δ 0.87 (6H, -C**H_3**) and δ 1.24, 1.25, 1.28, 1.54, 3.25, 3.30 (protons of two carbon chains). **^{13}C NMR** (400 MHz, $CDCl_3$): δ 14.13 (2C, -**C**H_3), 22.70 (2C, -**C**H_2CH_3), δ 41.31 (1C, Cl**C**H_2-$CONR_2$), δ 46.26, 48.33 (2C, -CON(**C**H2-$C_{17}H_{35})_2$) and δ 26.87, 26.92, 27.36, 29.15, 29.32,29.38,29.40,29.53,29.55, 29.57, 29.60, 29.63, 29.67, 29.71, 31.94 (30C, -**C**H_2 long chain carbons).

TOALH ligand. (2S,2'S)-1,1'-(1,4,7-triazonane-1,4-diyl)bis(propan-2-ol) (126 mg, 0.51 mmol) was dissolved in 100 ml of an acetonitrile : dichloromethane (70:30) mixture. To this solution, 245.8 mg (0.8Eq, 0.41 mmol) of N,N-distearoyl-2-chloro-acetamide and 4-5 equivalent DIPEA were added and the solution was stirred for 2 days at 70 °C. The reaction mixture was dried, dissolved in chloroform and washed with a 0.5 M sodium hydroxide solution. The chloroform layer was washed with water twice and then dried using anhydrous sodium sulfate, filtered and the filtrate was dried under reduced pressure to yield 2-(4,7-bis((S)-2-hydroxypropyl)-1,4,7-triazonan-1-yl)-N,N-dioctadecylacetamide, the TOAL ligand, as a solid in 98-99% yield with respect to the amount of N,N-distearoyl-2-chloro-acetamide reagent. The product was characterized using ESI-MS, ^{1}H NMR, ^{13}C NMR. A scheme for the synthesis of (2S,2'S)-1,1'-(1,4,7-triazonane-1,4-diyl)bis(propan-2-ol) and N,N-distearoyl-2-chloro-acetamide are shown in supplementary scheme S1. **ESI-MS:** m/z 808.02 ($M+H^+$, 100%), where M = TOAL ligand. The ESI-MS and NMR spectra are shown in the supporting information. **^{1}H NMR:** (400 MHz, $CDCl_3$): δ 5.34 (2H, -O**H**), δ 2.71 (4H, -C**H_2**-NH- hydroxypropyl alcohol pendants), δ 3.07, 2.89 (2H, -C**H** alcohol pendants), δ 3.20 (2H, -NHC**H_2**-$CONR_2$ amide pendant), δ 2.44 (12H, -C**H_2** macrocycle), δ 1.05 (6H, -C**H_3**) and δ 0.87, 1.24, 1.28, 1.39, 1.41, 1.49, 1.51, 1.64, 3.24, 3.28 (protons of two

long carbon chains). **^{13}C NMR** (400 MHz, $CDCl_3$): δ 14.10, 22.67 (2C, -**C**H_3), δ 51.01 (6C, macrocycle ring), δ 74.92, 70.34 (3C, -**C**H alcohol pendent), δ 67.34, 64.61 (3C, -**C**H_2-NH- alcohol pendents), and δ 37.81, 33.14, 31.91, 29.67, 29.35, 25.53 (15C, -**C**H_2 long chain carbon).

2.2.2. Synthesis of [Fe(TOAL-H$^+$)]Cl. The iron(III) complex was synthesized by dissolving the TOAL ligand (0.4 mmol) in 15 mL ethanol and heating the solution to 55-60 °C. Iron(II) chloride tetrahydrate (1.05 equivalent) was dissolved in ethanol (2-3 mL) and was added dropwise to the ethanolic ligand solution. The solution was allowed to stir for 2 days and the iron complex precipitated as a yellow solid. The iron complex was isolated by filtration and the resulting powder was washed with ethanol at room temperature. The iron complex was isolated as a brownish-orange solid in 85% yield. ESI-MS of [Fe(TOAL-H$^+$)].Cl^- : m/z = 861.56 [M^+], where M^+ = [Fe(TOAL-H$^+$)]$^+$. Fe content of the solid was determined using ICP-MS calculated for [Fe(TOAL-H+)]Cl: 6.24%, found: 6.46%.

2.2.3. Synthesis of TOABH. In a 50 mL round bottom, (2S,2'S)-1,1'-(1,4,7-triazonane-1,4-diyl)bis(propan-2-ol) (0.060 mmol) was dissolved in 10 mL absolute ethanol. The 2-chloro-N,N-dibenzylacetamide (0.075 mmol, 1.25 equiv.) was added to this solution along with five equivalents of sodium carbonate. The mixture was stirred at 70 °C for 16 hours. Sodium carbonate was removed via filtration and the ethanol was removed using a rotary evaporator. The resulting crude yellow oil was dissolved in 35 mL of 1 M HCl and washed with anhydrous ethyl ether (5 x 35 mL). The acidic solution was neutralized with NaOH pellets, dried to produce a yellow oil (Yield 49.5%), and then characterized using ESI-MS, ^{1}H NMR, ^{13}C NMR. **ESI-MS:** m/z 483.67 (M + H^+, 100%), 505.50 (M + Na^+, 10%) where M equals the TOAB ligand. **^{1}H NMR:** (500 MHz, MeOD): δ 1.04 (6H, -C**H**$_3$), δ 2.72, 3.86 (4H, -C**H**$_2$-NH- hydroxypropyl pendants), δ 2.98 (12H, -C**H**$_2$ macrocycle), δ 3.72 (2H, -C**H** hydroxypropyl pendants), δ 3.86 (2H, -C**H**$_2$-amide), δ 4.44, 4.58 (4H, -C**H**$_2$-benzyl), δ 7.32 (10H, -C**H** benzyl). **^{13}C NMR:** δ 17.01 (2C, **C**H_3), δ 49.10, 49.40 (2C, -**C**H_2-benzyl), δ 49.58, 50.05, 50.64, 51.18, 54.84 (6C, -**C**H_2 macrocycle), δ 56.93 (1C, -**C**H_2-amide), δ 62.73, 62.84 (2C, -**C**H_2 hydroxypropyl pendants), δ 63.20, 63.51 (2C, -**C**H

hydroxypropyl pendants), δ 126.25, 127.22, 127.40, 127.81, 128.36, 128.73 (10C, -**C**H, benzyl), δ 136.40, 136.86 (2C, -**C**- benzyl), δ 172.35 (1C, -**C**O).

2.2.4. Synthesis of [Fe(TOAB)]Br_2. The TOAB ligand (0.023 mmol) was dissolved in 3 mL of double distilled water. This solution was heated to 50 °C and the pH was monitored to ensure it was between 5.5 and 6.5. Iron (II) bromide anhydrous (0.023 mmol, 1 equivalent) was dissolved in 3 to 5 mL of double distilled water and added dropwise to the ligand solution. The solution was stirred for 18 hours after which time the water was removed using a rotary evaporator. The yellow oil was redissolved in 2 –3 mL of ethanol and a white solid was removed by centrifugation. To the dark orange ethanolic solution, 15 mL of anhydrous ethyl ether was added, to give a solid. The solid was collected via centrifugation and washed 3 times with ethyl ether to produce a light orange solid in 51% yield. **ESI-MS:** m/z 536.25 (M, 100%) where M^+ = $[Fe(TOAB\text{-}H^+)]^+$. Fe content of the solid was determined using ICP-MS calculated for [Fe(TOAB)]Br_2: 8.03%, found: 7.31%.

2.3 Magnetic susceptibility. The effective magnetic moments (μ_{eff},) of the Fe(III) complexes or paramagnetic liposomes were determined by ^{1}H NMR by using the Evans method.[41] Samples were prepared using a coaxial NMR insert which contained the diamagnetic standard of 5 % t-butanol in D_2O or $CDCl_3$. The effective magnetic moments of Fe(III) complexes is used to confirm molecular weight and to determine the concentration of Fe(III) complexes in the liposomes as reported previously.[26]

2.4 Liposome preparation and characterization.

2.4.1 Liposome Type A (LipoA) was prepared using the Mozafari method with some modification.[42] The hydration solution contained 40 mM of iron(III) complex at pH 6.8-6.9; with the pH adjusted using a 1 M NaOH solution and a total lipid concentration of 40 mM. The lipids were composed of DPPC : cholesterol : DSPE-PEG2000-NH_2 with a molar ratio of 77 : 15 : 8. First, cholesterol was added to a 1-dram glass vial with 3% (v/v) glycerol in the hydration solution, sealed with clear polyethylene film and capped in an airtight vial. This suspension was

stirred at 1000 rpm at 110-115 °C for 20 minutes, then the other two lipids were added and stirred at 60 °C for an hour, left standing without stirring at 55 °C for two hours and then cooled to room temperature without disturbing the solution. The resulting liposome suspension was passed 7-10 times at 60 °C through two sequentially stacked polycarbonate membranes of 400 nm pores using an Avanti mini-extruder with heating block. The 400 nm polycarbonate membranes were separated and supported by three 10 mm polyester drain discs by placing them alternately inside a mounting block of the extruder. After extrusion, the liposomal samples were allowed to cool to room temperature. The next extrusion process was carried out through 200 nm and then through 100 nm polycarbonate membranes to obtain 100 nm extruded liposomes following the same protocol and setup for 400 nm membrane. About 50 µL of extruded liposomes were removed for analysis by UV-vis spectrometry, ICP-MS and DLS prior to sample dialysis. The extruded liposomes were placed inside 10 KDa dialysis tubes for dialysis in solutions separately for 24 hours at 4 °C to wash away unencapsulated hydrophilic Iron complex present in the liposomal suspension at 300 mOsm/L NaCl. A Dynamic Light Scattering (DLS) instrument was used to measure the size and zeta potential of the liposomes by diluting 20 µL extruded liposomes in 300 mOsm/L aqueous solution. To measure the percent of encapsulated Fe(III) complex ($[Fe(NOTP)]^{3-}$), both UV-vis and ICP-MS techniques were used. For UV-vis, 20 µL of the non-extruded liposomes were isolated, diluted with 300 mOsm/L of NaCl aqueous solution to 1 ml, sealed and filtered using Amicon 100 KDa ultra-filtration kit at 70 psi argon pressure at room temperature. The filtrate was collected and analyzed by UV-vis spectrometry. The percent encapsulated iron complex was determined by comparing the absorbance at 250 nm of the initial hydration solution to that found in the filtrate by using an extinction coefficient of 5800 $M^{-1}cm^{-1}$ for Fe(NOTP). The Fe content was also determined by using ICP-MS. Approximately 1 mM 50 µL Fe(III) liposomal solution was made and digested in 60% nitric acid at 80 ^{o}C for two hours and then at room temperature for 3 days prior to subsequent dilutions for ICP-MS analysis. The details are reported previously.[43] All liposomes were stored at 4 °C.

2.4.2. Liposome type B (LipoB) was prepared by using the liposomal formulation composed of DPPC : DSPE-PEG2000-NH_2 : Cholesterol : Amphiphilic Fe(TOAL-H^+)Cl lipids with a molar ratio of 64 : 6 : 15 : 15 respectively. 100 nm LipoB solutions were formulated and prepared for analysis in a similar way to that of LipoA. However, the 2-hour period of standing without stirring was carried out in 60 °C instead of 55 °C and then the liposome was slowly cooled down to room temperature without disturbing the solution. The extrusion was carried out at 65 °C.

2.4.3. Liposome type C (LipoC) was prepared from DPPC : DSPE-PEG2000-NH_2 : Cholesterol : amphiphilic Fe(TOAL-H^+)Cl lipid with a molar ratio of 64 : 6 : 15 : 15 respectively, similar to LipoB. The hydration solution contained 40 mM of Na_3Fe(NOTP) complex at pH 6.8-6.9; with the pH adjusted with 1 M NaOH solution. The lipids were added to a 1-dram glass vial with 3% (v/v) glycerol in the hydration solution, sealed with clear polyethylene film and capped to an airtight vial. This suspension was stirred at 1000 rpm at 105-110 °C for 15 minutes, then stirred at 60 °C for an hour, left standing without stirring at 55 °C for two hours and then cooled to room temperature without disturbing the solution. 100 nm sized LipoC was formulated by using the extrusion and dialysis procedures described for LipoA.

2.4.4. Micelle preparation. The $[Fe(TOAL)]^{2+}$ micelles of 17 nm size were prepared by vortexing the $[Fe(TOAL)]^{2+}$ amphiphilic complexes in deionized water at room temperature and passing the suspension through a 450 nm syringe filter. The concentration of the amphiphilic complex in the micelle was calculated by using ICP-MS, and the micelle was size was characterized by using DLS.

2.5. Water proton relaxation times. Experiments were conducted at several magnetic field strengths including 1.4 T (34 ^oC), 4.7 T (37 ^oC) or at 9.4 T (37 ^oC). Sample concentrations were prepared by diluting iron liposomes. The samples were placed into a coaxial NMR tube insert and the NMR tube was filled with DMSO-d_6 as a reference. The T_1 proton relaxation times of solutions containing complex or liposomes were measured on a 9.4 T NMR spectrometer at 37 °C using the inversion recovery method with the following parameters: relaxation delay = 15-20

s, echo time array starting from 0.01 – 5 s. T_2 relaxation times were measured using the Carr–Purcell–Meiboom–Gill (CPMG) spin echo method. The CPMG sequence was used with a fixed TR of 10 - 15 s and TE times ranging from 0.02 – 10 ms in 12-24 exponential increments to 10-15s.

2.6. Mice imaging studies. In vivo, MR imaging was performed on at 4.7 T in accordance with approved Roswell Park IACUC protocols. Female mice were inoculated subcutaneously with CT26 colorectal cancer cell lines and tumors were allowed to grow to approximately 25 mm^3 (25.3 ± 7.8, mean ± SD). Solutions were formulated with Fe(III) complex loaded liposomes at 20-25 mg lipids/ml. Three-dimensional, spoiled gradient echo (SPGR) scans were acquired covering the upper thorax to the hindquarters with the following acquisition parameters: TE/TR/FA = 3/15/40°, FOV = 48x32x32 mm, acquisition matrix = 192x96x96, scan duration = 2.75 minutes. Sealed NMR tubes containing 1% agarose doped with 1mM and 2mM $CuSO_4$ were included for image signal normalization. A three-point standard intensity curve was previously generated over multiple imaging sessions using 2 phantoms and background noise and the signal intensities of datasets are linearly transformed to best fit standard intensity curve. Three pre-injection SPGR scans were acquired, contrast agent (50-125 µmol [Fe]/ kg intravenously via tail vein) was delivered intravenously via tail vein, then SPGR scans were acquired continuously up to 60’ after injection and 4 h later. Data sets were reconstructed to isotropic voxel sizes, frequency aliasing removed, and signal was normalized by phantom intensities using in-house analysis routines written in MATLAB (Mathworks, Natick MA). Regions of interest (ROIs) were created manually segmenting tumor, vessel (inferior vena cava), liver, renal cortex and urinary bladder using Analyze 10.0 (AnalyzeDirect, Overland Park KS). Signal intensities for post-injection scans were sampled for each ROI, and changes in intensities were calculated by subtraction of the average pre-injection intensity. For comparison, FDA-approved MRI contrast agent gadoterate meglumine (Gd-DOTA, Dotarem®) was injected at 100 µmol [Gd]/kg into a separate group of mice. Studies were carried out in duplicate (n=2) for each compound tested.

3. Results and discussion

3.1 Synthesis and characterization of Fe(III) complexes

The amphiphilic Fe(III) complex studied here was prepared from a macrocyclic ligand containing a pendant amide group substituted with two long (C18) hydrocarbon chains. The choice of a 1,4,7-triazacyclononane (TACN) macrocyclic ligand with hydroxypropyl pendants was inspired by previous studies that showed the formation of high spin Fe(III) complexes with relatively high proton relaxivity.[27-29] Such complexes with hydroxypropyl pendant groups may serve to increase the relaxivity at the Fe(III) center due to strong second-sphere interactions with water.[27] The Fe(III) complex of the new macrocyclic ligand, TOABH, was prepared in order to test the effect of mixed amide hydroxypropyl pendants on relaxivity in comparison to $[Fe(NOHP)]^{2+}$ which contains three hydroxypropyl pendants. This macrocycle was prepared by alkylation of bis-2-hydroxypropyl-1,4,7-triazacyclononane with N,N'-dibenzyl chloroacetamide. The dibenzyl amide was chosen to expedite synthesis as the macrocyclic ligand could be isolated by extraction into organic solvent. The amphiphilic macrocyclic ligand (TOALH) was prepared in an analogous procedure in good yield by alkylation of the macrocycle with N',N-distearoyl-2-chloroacetamide (Scheme S1, S2). The isolation of this ligand was facilitated by the addition of less than an equivalent of the pendant group, precipitation of the amphiphilic ligand and removal of excess macrocycle upon washing. The Fe(III) complex of TOAL was prepared by treatment of the amphiphilic ligand with $FeCl_2$ in organic solvent in the presence of air. This procedure is similar to that for analogous complexes that contain two or more hydroxypropyl pendants on 1,4,7-triazacyclononane (TACN).[27, 29] Such complexes readily oxidize to the high spin Fe(III) form. The Fe(III) complex of TOAB was prepared in water by addition of $FeBr_2$ to the ligand and adjustment of the pH to 5.5-6.5. The effective magnetic moments of $[Fe(TOAB)]^{2+}$ or $[Fe(TOAL)]^{2+}$ as measured by Evans method of magnetic susceptibility in water or in chloroform, respectively, are μ_{eff} = 6.1 ± 0.2 or 5.9 ±0.2, respectively, consistent with high spin Fe(III). The ^{1}H NMR spectrum of $[Fe(TOAB)]^{2+}$ (Figure S9) shows the absence of the paramagnetically shifted ligand proton resonances that are typically observed for alternative possibilities including Fe(III) low spin[44] or Fe(II) high spin complexes.[45]

Fe(III) complexes analogous to $[Fe(TOAB)]^{2+}$ that contain the TACN macrocycle and pendant hydroxypropyl groups are resistant to dissociation in 100 mM acid, or in serum as well

as in PBS buffer.[27, 29] The $[Fe(TOAB)]^{2+}$ complex similarly shows no evidence of dissociation at 37 ^{o}C in PBS buffer over a period of 72 hours (Figure S10) as shown by the lack of electronic absorbance changes. The electronic absorbance spectrum of the Fe(III) complex of TOAL is shown for comparison (Figure S11).

3.2 Preparation of paramagnetic liposomes and micelles

Pegylated liposomes of 95-125 nm size were prepared for LipoA, LipoB and LipoC as studied by dynamic Light Scattering (DLS). To encapsulate $[Fe(NOTP)]^{3-}$ in the liposomes, 40 mM solutions at pH 6.7-6.9 with HEPES buffer were used as the hydration medium, with the pH maintained at slightly acidic pH values to maintain solubility of the complex. For all liposomes the Mozafari method[42] was significantly easier to use for the preparation of small-sized liposomes by extrusion. The zeta potential of LipoA, LipoB and LipoC was -8 mV, +12 mV and +8 mV, respectively, in water. The stability of the liposomes was measured after a few days both in water and in the presence of serum by relaxivity (Table S2). These data showed that the liposomes were stable in saline solution and in mice serum. Further studies as a function of temperature are described below.

The $[Fe(TOAL)]^{2+}$ micelles of 17 nm size were prepared by vortexing the $[Fe(TOAL)]^{2+}$ amphiphilic complexes in water as shown in Figure S12. The critical micelle concentration is approximately 0.2 mM as shown by the plot of R_1 versus concentration of amphiphilic iron complex. The concentration of the amphiphilic complex in the micelle was calculated by using ICP-MS for iron.

3.3 Water proton relaxivity of complexes

The T_1 and T_2 water proton relaxation times were measured and the resulting relaxivity values for the iron complexes, $[Fe(NOTP)]^{3-}$ and $[Fe(TOAB)]^{2+}$ are given in Table 1. These small macrocyclic Fe(III) complexes have moderate proton relaxation values characteristic of analogous Fe(III) complexes that lack an inner-sphere water.[29, 37] Interestingly, $[Fe(TOAB)]^{2+}$ has decreased relaxivity compared to the analog with three hydroxypropyls ($[Fe(NOHP)]^{2+}$). Given that both complexes lack an inner-sphere water, the most likely cause of this unexpected

decrease is a change in the second-sphere water contribution to relaxivity by disruption of the coordination sphere by the two hydrophobic benzyl substituents on the amide group. Strong second-sphere water contributions likely produce the relatively high proton relaxation values for $[Fe(NOHP)]^{2+}$ in comparison to other closed coordination sphere complexes.[37] The substitution of hydroxypropyl pendants for phosphonate groups to form $[Fe(NOTP)]^{3-}$ also produces a decrease in relaxivity even though phosphonates are thought to promote second-sphere water contributions in MRI probes.[46] The magnetic field dependence of the three complexes from 1.4 to 9.4 T does not change markedly, although a slight dip is observed at 4.7 T for $[Fe(NOHP)]^{2+}$ and $[Fe(NOTP)]^{3-}$. Although studies of the full field strength relaxivity dependence are needed, it is interesting to note that NMRD profiles recently reported for EDTA derivatives of Fe(III) complexes,[14, 22] show a dispersion in r_1 from 10 MHz to 100 MHz with an increase at higher fields, a profile that is not very different than that observed here.

The T_1 and T_2 water proton relaxation times were measured for LipoA, LipoB and LipoC as a function of concentration of the iron complex in the liposome to obtain the relaxivities of the paramagnetic liposomes on a per iron and per particle basis as described (Table 1 and Table S3) As anticipated, the relaxivity values for the liposomal formulations vary substantially based on whether the iron complex is encapsulated or incorporated into the liposome. For LipoA, the encapsulated $[Fe(NOTP)]^{3-}$ complex shows quenched relaxivity in comparison to the free complex, suggesting limiting water exchange through the bilayer (r_1 = 0.65 versus 1.0 $mM^{-1}s^{-1}$).

The LipoB formulation has the highest relaxivity on a per iron basis of r_1 = 2.6 $mM^{-1}s^{-1}$ at 1.4 T. The amphiphilic complex in the outer lipid bilayer is positioned to interact with the bulk water protons, but the amphiphilic complexes in the inner bilayer have a quenched contribution. The inner versus outer complex contributions can be estimated using a reported approach that first estimates the permeability of the liposomal bilayer to water exchange.[47] From this approach and the graph in figure S21, it is clear that most of the relaxivity derives from the outer Fe(III) complexes in our liposomes because the liposomal water permeability is low. The relaxivity of LipoC, which contains both encapsulated and amphiphilic iron complexes is lower on a per iron basis given that the relaxivity of the encapsulated Fe(III) complexes is quenched. The per particle relaxivity of LipoC is similar at 7.8×10^3 $mM^{-1}s^{-1}$ compared to 2.6 ×

10^4 $mM^{-1}s^{-1}$ for LipoB as shown in Table S3. Values of r_1 in serum for LipoB and LipoC are compared to those in saline solution (Table 1). The relaxivity of micelles based on the amphiphilic Fe(III) complex of TOAL (size of 17 nm) is 2.6 $mM^{-1}s^{-1}$ based on iron content when measured at 1.4 T and 34 °C and neutral pH (Figure S12).

These data show that there is a nearly four-fold increase in the r_1 values per iron for the micellar probe in comparison to $Fe(TOAB)]^{2+}$. It is interesting to consider the basis for this increase. The proton relaxivity of the iron centers in all complexes here (Figure 1) are attributed to second-sphere water contributions which typically have short residence times, on the picosecond time scale. Moreover for the small molecules, $[Fe(TOAB)]^{2+}$ and $[Fe(NOHP)]^{2+}$, rotational correlation times are also expected to be short (≈ 100 ps) so that both rotational motion and second-sphere contributions may be limiting for producing proton relaxation.[48] The increase in the r_1 on a per iron basis may be attributed to a decrease in rotational correlation times in the micelles and perhaps also a change in the second-sphere water residence times. Both liposomes and micelles are known to have rotational times on the order of nanoseconds and produce an increase in r_1 in comparison to the small molecule MRI probe for probes that have inner-sphere or second-sphere water contributions to relaxivity.[48] The linker flexibility is also important in the production of larger relaxivities, with more rigid linkers functioning best.[47] The amphiphilic complex used here has the two alkyl chains incorporated directly into the pendant group which is expected to give a rigid connection directly to the bound pendant group. Other factors that may influence the relaxation of the Fe(III) complex in the micelles or in the liposomes include the interaction with bulk water. Whereas the small molecule complexes interact freely with water, the Fe(III) center in the liposome may be influenced by the lipids or by the neighboring Fe(III) centers.

The r_2 values for liposomes with amphiphilic Fe(III) such as LipoB increase markedly at higher field strengths (9.4 T), similar to observations in previous reports of lanthanide(III) based liposomal systems.[8] The increase of T_2 relaxation rate constants with increasing field strength is based on the known field strength dependence of the magnetic susceptibility contribution to r_2. As shown here, the r_2/r_1 ratio for LipoB increases from 1.5 at 1.4 T to 6.9 at 9.4 T.[8] Such increased r_2/r_1 ratios are not favorable for detection of paramagnetic liposomes, although the

field strengths that showed the most dramatic increases here are higher than those used for human clinical imaging.

Table 1. Relaxivity values for Fe(III)-based liposomes and complexes

AGENT	r_1 ($mM^{-1}s^{-1}$) 1.4 T	r_2 ($mM^{-1}s^{-1}$) 1.4 T	r_1 ($mM^{-1}s^{-1}$) 4.7 T	r_2 ($mM^{-1}s^{-1}$) 4.7 T	r_1 ($mM^{-1}s^{-1}$) 9.4 T	r_2 ($mM^{-1}s^{-1}$) 9.4 T
Fe(NOTP)	1.0[a]	1.4	0.72[a]	1.3[a]	0.86[a]	1.4
With HSA	(1.3)[a]	(1.5)	(1.0)[a]	(1.6)[a]	(1.2)	(1.3)
Fe(TOAB)[b]	0.66	1.1	-	-	0.65	2.5
With HSA	(0.85)	(1.2)			(1.2)	(2.7)
Fe(NOHP)	1.5[a]	1.8	0.97[a]	1.8[a]	1.4[a]	2.1
With HSA	(1.5)[a]	(2.1)	(1.2)[a]	(2.3)[a]	(1.4)	(1.9)
LipoA	0.65	0.89	-	-	0.67	4.9
Serum	(0)	(0.82)	-	-	(0.65)	(2.6)
LipoB	2.6	4.0	-	-	2.8	19
Serum	(2.6)	(2.6)			(2.2)	(9.8)
LipoC	0.58	1.7	-	-	0.93	5.5
Serum	(1.2)	(3.7)			(2.4)	(8.5)

The r_1 and r_2 in buffered aqueous solution are reported at 4.7 T, 9.4 T (37 °C) and 1.4 T (34 °C), pH 6.8-7.2 with r_1 and r_2 relaxivities in serum reported in parenthesis. Standard deviations for r_1 and r_2 values are < 20%. a) values from reference[37] b) meglumine was added to adjust pH to the listed range to maintain solubility.

Temperature dependent studies of T_1 proton relaxation times show a modest decrease in relaxation rate constants as temperature is raised from 25 °C to 65 °C for LipoA, LipoB and LipoC (Figure S14). These studies were carried out as another test of liposome stability as well as to more fully characterize the liposomal agents. The decrease in relaxation rate constant with temperature is typical behavior for a paramagnetic complex where water exchange in not rate limiting[49,40] which is the case here as the complexes do not have an inner-sphere water. One might expect that these liposomal agents would show an increase in relaxation rates with

temperature as water exchange through the lipid bilayer increases. However, the contribution from water exchange through the lipid bilayer is small. Similar temperature dependencies have been observed for Fe(III) complexes containing hydroxpropyl pendants that lack an exchangeable water ligand and rely on second-sphere relaxivity contributions.[50] Both LipoA and LipoC show a modest increase in relaxation rate constants upon returning to the initial temperature after heating. The slightly higher values that are measured as the liposomes are cooled back down to 25 °C are consistent with the release of a small percentage of the iron complex from LipoA and LipoC upon incubation at high temperatures. Consistent with these studies, the incubation of LipoA and LipoC at 37 °C in saline followed by centrifugation and measurement of leaked $[Fe(NOTP)]^{3-}$ showed 6.1 % and 9.2% leakage after four days respectively.

3.4 MRI studies in BALB/c mice

LipoA, LipoB and LipoC were studied at doses of 110, 230 and 210 mg lipid/kg (55, 50 and 100 μmol Fe/kg, respectively), in BALB/c mice containing subcutaneous CT26 tumors with the goal of monitoring the pharmacokinetic clearance and enhanced contrast from each liposome formulation (Figures 3-5 and Figures S15-17). PEGylated liposomes such as LipoA, LipoB or LipoC typically show increased circulation times (2-15 h) in animals due to decreased rates of hepatobiliary elimination.[1] As shown in Figure 3 and 5, LipoB shows more highly enhanced contrast in the vena cava and long circulation times in the blood pool, suggesting that it does not readily escape the vasculature. Lower volumes of distribution (V_d) and non-renal elimination were observed for LipoB over four hours compared to the other two agents (Table S3). LipoB shows enhanced kidney signal (Figure S16) but did not appear to be excreted through the bladder over 40 minutes period unlike LipoA and LipoC. Within 4 hours, LipoB is eliminated through hepatobiliary system as observed by sustained gall bladder enhancement (Figure S16).

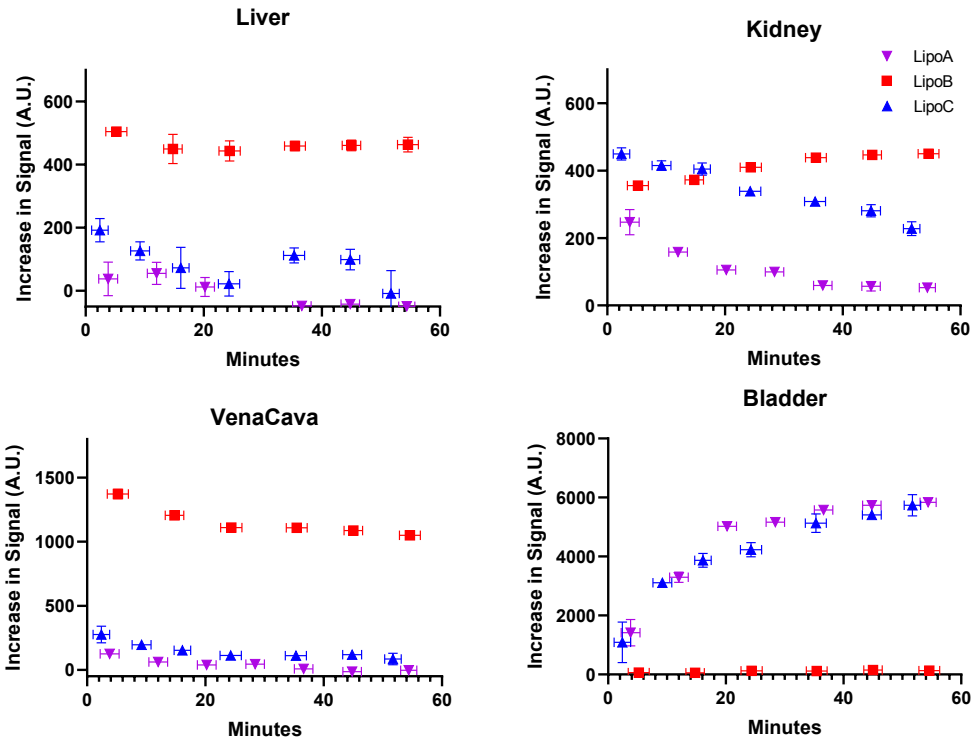

Figure 3. Changes in T_1-weighted signal intensity for LipoA (55 µmol [Fe] /kg), LipoB (50 µmol [Fe] /kg), or LipoC (100 µmol [Fe] /kg) over time in blood (vena cava), kidneys, liver or urinary bladder in BALB/c mice with CT26 tumors.

LipoA and LipoC show reduced contrast in the vena cava and enhanced contrast in the kidney and bladder over a period of 40 minutes. The contrast enhancement in the bladder is consistent with the leakage of $[Fe(NOTP)]^{3-}$ from these liposomes followed by renal clearance. This data is consistent with studies showing that liposomes loaded with $[Fe(NOTP]^{3-}$ complex are less stable than liposomes with only the amphiphilic complex in serum. Positively charged LipoB has a half-life of 70 minutes, which is lower than that of typical neutral or negatively charged liposomes.[51] This increased clearance rate may be a result of blood protein absorption and binding to erythrocytes. Our previous studies that featured liposomes with both amphiphilic and the encapsulated complex, $[Fe(NOHP)]^{2+}$ also showed partial renal clearance attributed to release of the complex from the liposomal interior.

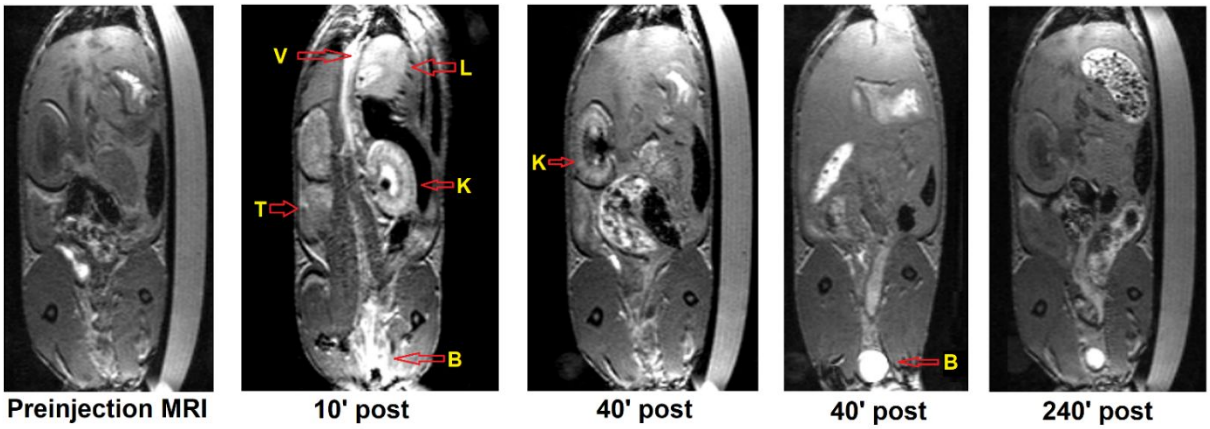

Figure 4. MR image of biodistribution and elimination of LipoC in a CT26 tumored BALB/c mouse. Dose was 125 µmol [Fe] /kg or 230 mg lipid/kg lipids per mouse body weight. Vena cava (V), Tumor (T), Liver (L), Kidney (K) and Bladder (B) are highlighted in post-injection MR images.

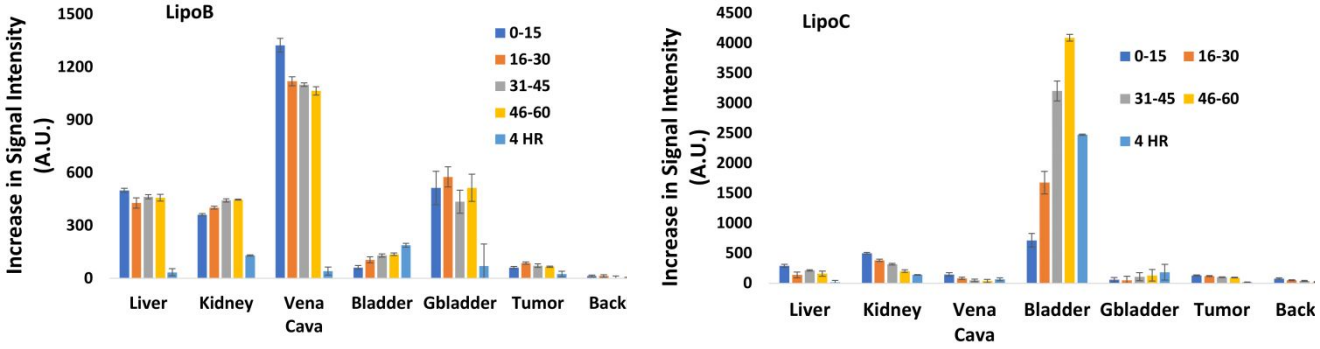

Figure 5. Changes in T_1-weighted signal intensity over time for LipoB (50 µM Fe/kg and LipoC (120 µM Fe /kg) in BALB/c mice with CT26 tumors.

The change in T_1 weighted signal intensity produced by LipoB and LipoC in murine CT26 tumors was examined, but the signal was low for both liposomal formulations (Figure 5). Comparison with the change in signal in the vena cava over time was made to determine whether the tumor signal could be attributed to tumor accumulation. A plot of the signal in tumor compared to that in the vena cava showed a small increase over the 40-minute time-period which is consistent with tumor uptake (Figure S18). Moreover for LipoB, signal

enhancement within the vena cava decreased from an 152% (45-60' post injection) enhancement to 6% enhancement at 4hrs, (96% decrease), while tumor decreased from a 15% MR signal enhancement to ~6% signal enhancement, at decrease of only 60%, supporting tumor accumulation. However, the contrast enhancement is small and further studies will require liposomes with higher relaxivity for studies of tumor imaging.

4. Conclusions

This research shows that an amide pendant group with two alkyl chains can be used to form an amphiphilic Fe(III) complex that inserts into a micellar aggregate or liposome. Modification of an amide group is a common and convenient synthetic route to prepare ligands for conjugation. However, somewhat surprisingly, the substitution of an amide for a hydroxypropyl pendant produced a complex with lowered relaxivity in comparison to the symmetrically substituted Fe(III) complex. This is most likely due to a disruption in the hydrogen bonding in the coordination sphere and corresponding change in second-sphere water contributions to relaxivity. However, we cannot rule out a change in zero-field splitting from changes in coordination environment and a corresponding change in electronic relaxation times[14] for the two Fe(III) complexes.

Incorporation of the Fe(III) complex into a micelle or liposome substantially increased the MRI probe relaxivity. Thus, the amphiphilic Fe(III) complex of TOAL, shows a four-fold greater r_1 per Fe(III) when incorporated into the micelle in comparison to the free complex, $[Fe(TOAB)]^{2+}$, in buffered aqueous solutions. In comparison, our previous studies showed little improvement in r_1 for liposomes containing amphiphilic complex, $[Fe(NOHPL)]^{2+}$compared to hydrophilic small molecule complex $[Fe(NOHP)]^{2+}$, with values of 1.7 and 1.5 $mM^{-1}s^{-1}$ per iron center at 1.4 T, 34 ^{o}C, respectively. However this study was more limited and did not include micelles or liposomes containing only amphiphilic Fe(III) complex, thus a direct comparison is difficult. In order to further increase r_1 from iron-based liposomes, future studies will focus on Fe(III) complexes with an inner-sphere water that have higher relaxivity values. For example, analogous Fe(III) complexes with a TACN framework, two hydroxypropyl groups and a bound

water show relaxivities of three to four-fold higher than $[Fe(TOAB)]^{2+}$,[27, 29] but these derivatives are often more difficult to prepare. In addition for Fe(III) complexes with an inner-sphere water ligand, it is important to choose pendant groups that prevent the formation of hydroxy or oxo-bridged dimers.[30]

The lower solubility of Fe(III) complexes is another challenge that must be overcome to prepare encapsulated liposomes. Hydration solutions of 40 mM $[Fe(NOTP)]^{3-}$ complex were used to form LipoA and LipoC formulations although higher solubilities (≈ 100 mM) could be obtained at more acidic pH values (6.0) with addition of buffer. This iron complex solubility is less than that of Gd(III) complexes that are used in hydration solutions of 300 mM. On the other hand, amphiphilic complexes of Fe(III) were loaded into the bilayer at 15% lipid content. Thus, the attachment of an amphiphilic tail for incorporation into a liposome of micelle is one approach to bypass the lowered aqueous solubility of Fe(III) complex MRI probes.

The apparent difference in the stability of Lipo B compared to the LipoC formulations in vivo was remarkable. Both liposomes were stable in saline and serum for a few days at 25 °C as shown by relaxivity studies. However, there were some indications that LipoC was less stable as shown by release of a few percent $[Fe(NOTP)]^{3-}$ from the liposomes after several days. In vivo, LipoB produced strong signal in the vasculature for over an hour. The LipoC formulation was apparently less stable in vivo and showed probe clearance through the kidney with a correspondingly large signal in the bladder that was consistent with release of $[Fe(NOTP)]^{3-}$. LipoA formulations were stable in solutions containing saline or serum have lowered relaxivity, consistent with the quenching of relaxivity by the liposome and restricted water exchange which produced low levels of enhanced contrast in mice MRI studies.

LipoC contains both amphiphilic and encapsulated iron complex and constitutes a type of dual MRI probe. The amphiphilic complex increases the probe relaxivity as the iron complex on the outer layer of the liposome is positioned to interact with the bulk water. On the other hand, liposomes carrying encapsulated paramagnetic complexes are often used as a type of responsive probe.[32, 52] The paramagnetic metal complex may be released by ultrasound waves and/or heating, pH changes or light. For example, liposomes are taken up into tumors and the

probe is released through heating to study the release of a hydrophilic molecule to the tumor.[53] We envision that the dual probes developed here may find application in cases where the amphiphilic and encapsulated probes produce signals that can be distinguished, for example by different r_1/r_2 values for contrast agents of different sizes.[54] However, the stability of the dual MRI probes such as lipoC must be increased for these future applications.

Conflicts of Interest

JRM is a co-founder of Ferric Contrast, Inc, a company that develops iron-based contrast agents.

Ethical Statement

All animal procedures were performed in accordance with the Guidelines for Care and Use of Laboratory Animals of the National Research Council of the US National Academies, 8th edition and approved by Roswell Park's Institutional Animal Care and Use Committee (IACUC).

Acknowledgments

JRM thanks the NSF (CHE-2004135) for support of this research. JAS acknowledges Roswell Park's Comprehensive Cancer Center Support Grant (P30CA016056). The authors would like to thank the Chemistry Instrument Center, and Magnetic Resonance Center at the University at Buffalo. This work utilized ICP-MS and FTMS that was purchased with funding from a NSF Major Research Instrumentation Program (NSF CHE-0959565) and the Bruker 500 MHz NMR (NSF CHE-2018160). We thank Professor Javid Rzayev for providing access to the DLS instrument and John Pinti for initial studies on liposomal agents.

References

(1) Langereis, S.; Geelen, T.; Grull, H.; Strijkers, G. J.; Nicolay, K. Paramagnetic liposomes for molecular MRI and MRI-guided drug deliveryc (vol 26, pg 728, 2013). *NMR Biomed* **2013**, *26* (9), 1195-1195.
(2) Mulder, W. J. M.; Strijkers, G. J.; van Tilborg, G. A. F.; Griffioen, A. W.; Nicolay, K. Lipid-based nanoparticles for contrast-enhanced MRI and molecular imaging. *Nmr Biomed* **2006**, *19* (1), 142-164.
(3) a) Castelli, D. D.; Gianolio, E.; Crich, S. G.; Terreno, E.; Aime, S. Metal containing nanosized systems for MR-Molecular Imaging applications. *Coordin Chem Rev* **2008**, *252* (21-22), 2424-2443. b) Crich, S. G.; Terreno, E.; Aime, S. Nano-sized and other improved reporters for magnetic resonance imaging of angiogenesis. *Adv Drug Deliver Rev* **2017**, *119*, 61-72.
(4) Strijkers, G. J.; Mulder, W. J.; van Heeswijk, R. B.; Frederik, P. M.; Bomans, P.; Magusin, P. C.; Nicolay, K. Relaxivity of liposomal paramagnetic MRI contrast agents. *MAGMA* **2005**, *18* (4), 186-192.
(5) Mulder, W. J.; Strijkers, G. J.; Griffioen, A. W.; van Bloois, L.; Molema, G.; Storm, G.; Koning, G. A.; Nicolay, K. A liposomal system for contrast-enhanced magnetic resonance imaging of molecular targets. *Bioconjug Chem* **2004**, *15* (4), 799-806.
(6) Guyon, L.; Groo, A. C.; Malzert-Freon, A. Relevant Physicochemical Methods to Functionalize, Purify, and Characterize Surface-Decorated Lipid-Based Nanocarriers. *Mol Pharmaceut* **2021**, *18* (1), 44-64.
(7) Mulder, W. J.; Strijkers, G. J.; Habets, J. W.; Bleeker, E. J.; van der Schaft, D. W.; Storm, G.; Koning, G. A.; Griffioen, A. W.; Nicolay, K. MR molecular imaging and fluorescence microscopy for identification of activated tumor endothelium using a bimodal lipidic nanoparticle. *FASEB J* **2005**, *19* (14), 2008-2010.
(8) Mulas, G.; Ferrauto, G.; Dastru, W.; Anedda, R.; Aime, S.; Terreno, E. Insights on the relaxation of liposomes encapsulating paramagnetic Ln-based complexes. *Magn Reson Med* **2015**, *74* (2), 468-473.
(9) Aime, S.; Castelli, D. D.; Lawson, D.; Terreno, E. Gd-loaded liposomes as T-1, susceptibility, and CEST agents, all in one. *J Am Chem Soc* **2007**, *129* (9), 2430-31.
(10) a) Do, Q. N.; Ratnakar, J. S.; Kovacs, Z.; Sherry, A. D. Redox- and Hypoxia-Responsive MRI Contrast Agents. *Chemmedchem* **2014**, *9* (6), 1116-1129. b) Major, J. L.; Meade, T. J. Bioresponsive, cell-penetrating, and multimeric MR contrast agents. *Acc Chem Res* **2009**, *42* (7), 893-903. c) Shuvaev, S.; Akam, E.; Caravan, P. Molecular MR Contrast Agents. *Invest Radiol* **2021**, *56* (1), 20-34.
(11) Gupta, A.; Caravan, P.; Price, W. S.; Platas-Iglesias, C.; Gale, E. M. Applications for transition-metal chemistry in contrast-enhanced magnetic resonance imaging. *Inorg Chem* **2020**, *59* (10), 6648-6678.
(12) Kras, E. A.; Snyder, E. M.; Sokolow, G. E.; Morrow, J. R. The Distinct Coordination Chemistry of Fe(III)-based MRI Probes. *Acc. Chem. Res.* **2022**, *55*, 1435-1444.
(13) Morrow, J. R.; Raymond, J. J.; Chowdhury, M. S. I.; Sahoo, P. R. Redox-Responsive MRI Probes Based on First-Row Transition-Metal Complexes. *Inorg Chem* **2022**, *61* (37), 14487-14499.
(14) Baranyai, Z.; Carniato, F.; Nucera, A.; Horvath, D.; Tei, L.; Platas-Iglesias, C.; Botta, M. Defining the conditions for the development of the emerging class of Fe(III)-based MRI contrast agents *Chem. Sci.* **2021**, *12*, 11138-11145.
(15) Botta, M.; Carniato, F.; Esteban-Gómez, D.; Platas-Iglesias, C.; Tei, L. Mn (II) compounds as an alternative to Gd-based MRI probes. *Future med chem* **2019**, *11* (12), 1461-1483.
(16) Wahsner, J.; Gale, E. M.; Rodriguez-Rodriguez, A.; Caravan, P. Chemistry of MRI Contrast Agents: Current Challenges and New Frontiers. *Chem Rev* **2019**, *119* (2), 957-1057.
(17) Hu, M. Y.; Chen, J.; Wang, J. M.; Zhang, Y.; Liu, L.; Morais, P. C.; Bi, H. Cu2+-Complex of hydrophilic nitrogen-rich polymer dots applied as a new MRI contrast agent. *Biomater Sci-Uk* **2017**, *5* (11), 2319-2327.
(18) a) O'Neill, E. S.; Kaur, A.; Bishop, D. P.; Shishmarev, D.; Kuchel, P. W.; Grieve, S. M.; Figtree, G. A.; Renfrew, A. K.; Bonnitcha, P. D.; New, E. J. Hypoxia-Responsive Cobalt Complexes in Tumor Spheroids: Laser Ablation Inductively Coupled Plasma Mass Spectrometry and Magnetic Resonance Imaging Studies. *Inorg Chem* **2017**, *56* (16), 9860-9868. b) Dunbar, L.; Sowden, R. J.; Trotter, K. D.; Taylor, M. K.; Smith, D.; Kennedy, A. R.; Reglinski, J.; Spickett, C. M. Copper complexes as a source of redox active MRI contrast agents. *Biometals* **2015**, *28* (5), 903-912.

(19) Theil, E. C. Ferritin: The Protein Nanocage and Iron Biomineral in Health and in Disease. *Inorganic Chemistry* **2013**, *52* (21), 12223-12233.
(20) a) Gale, E. M.; Atanasova, I. P.; Blasi, F.; Ay, I.; Caravan, P. A manganese alternative to gadolinium for MRI contrast. *J Am Chem Soc* **2015**, *137* (49), 15548-15557. b) Wang, J.; Wang, H.; Ramsay, I. A.; Erstad, D. J.; Fuchs, B. C.; Tanabe, K. K.; Caravan, P.; Gale, E. M. Manganese-Based Contrast Agents for Magnetic Resonance Imaging of Liver Tumors: Structure-Activity Relationships and Lead Candidate Evaluation. *J Med Chem* **2018**, *61* (19), 8811-8824.
(21) a) Lauffer, R. B. Paramagnetic metal complexes as water proton relaxation agents for NMR imaging: theory and design. *Chem Rev* **1987**, *87* (5), 901-927. b) Schwert, D. D.; Richardson, N.; Ji, G.; Radüchel, B.; Ebert, W.; Heffner, P. E.; Keck, R.; Davies, J. A. Synthesis of two 3, 5-disubstituted sulfonamide catechol ligands and evaluation of their iron (III) complexes for use as MRI contrast agents. *J med chem* **2005**, *48* (23), 7482-7485. Kuźnik, N.; Wyskocka, M. Iron (III) contrast agent candidates for MRI: a survey of the structure–effect relationship in the last 15 years of studies. *Eur J Inorg Chem* **2016**, *2016* (4), 445-458.
(22) Uzal-Varela, R.; Lucio-Martinez, F.; Nucera, A.; Botta, M.; Esteban-Gomez, D.; Valencia, L.; Rodriguez-Rodriguez, A.; Platas-Iglesias, C. A systematic investigation of the NMR relaxation properties of Fe(iii)-EDTA derivatives and their potential as MRI contrast agents. *Inorg Chem Front* **2023**, *10* (5), 1633-1649.
(23) a) Wang, H.; Jordan, V. C.; Ramsay, I. A.; Sojoodi, M.; Fuchs, B. C.; Tanabe, K. K.; Caravan, P.; Gale, E. M. Molecular magnetic resonance imaging using a redox-active iron complex. *J Am Chem Soc* **2019**, *141* (14), 5916-5925. b) Xie, J.; Haeckel, A.; Hauptmann, R.; Ray, I. P.; Limberg, C.; Kulak, N.; Hamm, B.; Schellenberger, E. Iron(III)-tCDTA derivatives as MRI contrast agents: Increased T-1 relaxivities at higher magnetic field strength and pH sensing. *Magn Reson Med* **2021**, *85* (6), 3370-3382. c) Palagi, L.; Di Gregorio, E.; Costanzo, D.; Stefania, R.; Cavallotti, C.; Capozza, M.; Aime, S.; Gianolio, E. Fe(deferasirox)2: An Iron(III)-Based Magnetic Resonance Imaging T1 Contrast Agent Endowed with Remarkable Molecular and Functional Characteristics. *J Am Chem Soc* **2021**, *143* (35), 14178-14188. d) Karbalaei, S.; Franke, A.; Jordan, A.; Rose, C.; Pokkuluri, P. R.; Beyers, R. J.; Zahl, A.; Ivanovic-Burmazovic, I.; Goldsmith, C. R. A Highly Water- and Air-Stable Iron-Containing MRI Contrast Agent Sensor for H2O2. *Chem-Eur J* **2022**, *28* (46). DOI: ARTN e202201179; 10.1002/chem.202201179.
(24) Botta, M.; Geraldes, C. F. G. C.; Tei, L. High spin Fe(III)-doped nanostructures as T-1 MR imaging probes. *Wires Nanomed Nanobi* **2023**, *15* (2). DOI: 10.1002/wnan.1858.
(25) Morrow, J. R. C., M. S. I.; Abozeid, S. M.; Patel, A.; Raymond, J. J. Transition metal ParaCEST, LipoCEST and CellCEST agents as MRI probes. In *Encyclopedia of Inorganic and Bioinorganic Chemistry*; Storr, R. A. S. a. T., Ed.; John Wiley & Sons, 2020; pp 1-19.
(26) Abozeid, S. M.; Asik, D.; Sokolow, G. E.; Lovell, J. F.; Nazarenko, A. Y.; Morrow, J. R. CoII Complexes as Liposomal CEST Agents. *Angew Chem Int Ed* **2020**, *132* (29), 12191-12195.
(27) Snyder, E. M.; Asik, D.; Abozeid, S. M.; Burgio, A.; Bateman, G.; Turowski, S. G.; Spernyak, J. A.; Morrow, J. R. A Class of FeIII Macrocyclic Complexes with Alcohol Donor Groups as Effective T1 MRI Contrast Agents. *Angew Chem Int Ed* **2020**, *132* (6), 2435-2440.
(28) Asik, D.; Abozeid, S. M.; Turowski, S. G.; Spernyak, J. A.; Morrow, J. R. Dinuclear Fe(III) Hydroxypropyl-Appended Macrocyclic Complexes as MRI Probes. *Inorg Chem* **2021**, *60* (12), 8651-8664.
(29) Asik, D.; Smolinski, R.; Abozeid, S. M.; Mitchell, T. B.; Turowski, S. G.; Spernyak, J. A.; Morrow, J. R. Modulating the properties of Fe (III) macrocyclic MRI contrast agents by appending sulfonate or hydroxyl groups. *Molecules* **2020**, *25* (10), 2291.
(30) Wang, H.; Wong, A.; Lewis, L. C.; Nemeth, G. R.; Jordan, V. C.; Bacon, J. W.; Caravan, P.; Shafaat, H. S.; Gale, E. M. Rational Ligand Design Enables pH Control over Aqueous Iron Magnetostructural Dynamics and Relaxometric Properties. *Inorganic Chemistry* **2020**, *59* (23), 17712-17721.

(31) Schwendener, R. A.; Wuthrich, R.; Duewell, S.; Wehrli, E.; Vonschulthess, G. K. A Pharmacokinetic and Mri Study of Unilamellar Gadolinium-Dtpa-Stearate, Manganese-Dtpa-Stearate, and Iron-Dtpa-Stearate Liposomes as Organ-Specific Contrast Agents. *Invest Radiol* **1990**, *25* (8), 922-932.
(32) Kneepkens, E.; Fernandes, A.; Nicolay, K.; Grull, H. Iron(III)-Based Magnetic Resonance-Imageable Liposomal T1 Contrast Agent for Monitoring Temperature-Induced Image-Guided Drug Delivery. *Invest Radiol* **2016**, *51* (11), 735-745.
(33) Li, Y. N.; Cong, H. L.; Wang, S.; Yu, B.; Shen, Y. Q. Liposomes modified with bio-substances for cancer treatment. *Biomater Sci-Uk* **2020**, *8* (23), 6442-6468.
(34) Laurent, S.; Elst, L. V.; Thirifays, C.; Muller, R. N. Paramagnetic liposomes: inner versus outer membrane relaxivity of DPPC liposomes incorporating lipophilic gadolinium complexes. *Langmuir* **2008**, *24* (8), 4347-4351.
(35) Fossheim, S. L.; Fahlvik, A. K.; Klaveness, J.; Muller, R. N. Paramagnetic liposomes as MRI contrast agents: Influence of liposomal physicochemical properties on the in vitro relaxivity. *Magn Reson Imaging* **1999**, *17* (1), 83-89.
(36) Ghaghada, K. B.; Ravoori, M.; Sabapathy, D.; Bankson, J.; Kundra, V.; Annapragada, A. New Dual Mode Gadolinium Nanoparticle Contrast Agent for Magnetic Resonance Imaging. *Plos One* **2009**, *4* (10). DOI: ARTN e7628; 10.1371/journal.pone.0007628.

(37) Kras, E. A.; Abozeid, S. M.; Eduardo, W.; Spernyak, J. A.; Morrow, J. R. Comparison of phosphonate, hydroxypropyl and carboxylate pendants in Fe(III) macrocyclic complexes as MRI contrast agents. *J Inorg Biochem* **2021**, *225*, 111594. DOI: 10.1016/j.jinorgbio.2021.111594.
(38) Patel, A.; Asik, D.; Snyder, E. M.; Delillo, A. E.; Cullen, P. J.; Morrow, J. R. Binding and release of Fe (III) complexes from glucan particles for delivery of T1 MRI contrast agents. *Chemmedchem* **2020**, *15*, 1050-1057.
(39) Bernier, D.; Blake, A. J.; Woodward, S. Improved procedure for the synthesis of enamine N-oxides. *J Org Chem* **2008**, *73* (11), 4229-4232. DOI: 10.1021/jo8002166 From NLM PubMed-not-MEDLINE.
(40) Abozeid, S. M.; Snyder, E. M.; Tittiris, T. Y.; Steuerwald, C. M.; Nazarenko, A. Y.; Morrow, J. R. Inner-sphere and outer-sphere water interactions in Co (II) paraCEST agents. *Inorg Chem* **2018**, *57* (4), 2085-2095.
(41) Schubert, E. M. Utilizing the Evans Method with a Superconducting Nmr Spectrometer in the Undergraduate Laboratory. *J Chem Educ* **1992**, *69* (1), 62-62. DOI: DOI 10.1021/ed069p62.1. Piguet, C. Paramagnetic susceptibility by NMR: The ''solvent correction'' removed for large paramagnetic molecules. *J Chem Educ* **1997**, *74* (7), 815-816. DOI: DOI 10.1021/ed074p815.
(42) Mozafari, R. M. *Nanoliposomes: from fundamentals to recent developments*; Trafford, 2005.
(43) Asik, D.; Smolinski, R.; Abozeid, S. M.; Mitchell, T. B.; Turowski, S. G.; Spernyak, J. A.; Morrow, J. R. Modulating the Properties of Fe(III) Macrocyclic MRI Contrast Agents by Appending Sulfonate or Hydroxyl Groups. *Molecules* **2020**, *25* (10), 2291.
(44) Tsitovich, P. B.; Gendron, F.; Nazarenko, A. Y.; Livesay, B. N.; Lopez, A. P.; Shores, M. P.; Autschbach, J.; Morrow, J. R. Low-Spin Fe(III) Macrocyclic Complexes of Imidazole-Appended 1,4,7-Triazacyclononane as Paramagnetic Probes. *Inorg Chem* **2018**, *57* (14), 8364-8374.
(45) Dorazio, S. J.; Tsitovich, P. B.; Siters, K. E.; Spernyak, J. A.; Morrow, J. R. Iron(II) PARACEST MRI Contrast Agents. *J Am Chem Soc* **2011**, *133* (36), 14154-14156.
(46) Botta, M. Second coordination sphere water molecules and relaxivity of gadolinium (III) complexes: implications for MRI contrast agents. *Eur J Inorg Chem* **2000**, *2000* (3), 399-407.
(47) Cittadino, E.; Botta, M.; Tei, L.; Kielar, F.; Stefania, R.; Chiavazza, E.; Aime, S.; Terreno, E. In Vivo Magnetic Resonance Imaging Detection of Paramagnetic Liposomes Loaded with Amphiphilic Gadolinium(III) Complexes: Impact of Molecular Structure on Relaxivity and Excretion Efficiency. *Chempluschem* **2013**, *78* (7), 712-722.

(48) Botta, M.; Tei, L. Relaxivity Enhancement in Macromolecular and Nanosized GdIII-Based MRI Contrast Agents. *Eur J Inorg Chem* **2012**, (12), 1945-1960.
(49) a) Aime, S.; Barge, A.; Botta, M.; Parker, D.; DeSousa, A. S. Prototropic vs whole water exchange contributions to the solvent relaxation enhancement in the aqueous solution of a cationic Gd3+ macrocyclic complex. *J Am Chem Soc* **1997**, *119* (20), 4767-4768. b) Pierre, V. r. C.; Allen, M. J.; Royal Society of Chemistry (Great Britain). *Contrast agents for MRI : experimental methods*; Royal Society of Chemistry, 2018.
(50) Abozeid, S. M.; Chowdhury, M. S. I.; Asik, D.; Spernyak, J. A.; Morrow, J. R. Liposomal Fe(III) Macrocyclic Complexes with Hydroxypropyl Pendants as MRI Probes. *Acs Appl Bio Mater* **2021**, *4* (11), 7951-7960.
(51) Campos-Martorell, M.; Cano-Sarabia, M.; Simats, A.; Hernandez-Guillamon, M.; Rosell, A.; Maspoch, D.; Montaner, J. Charge effect of a liposomal delivery system encapsulating simvastatin to treat experimental ischemic stroke in rats. *Int J Nanomed* **2016**, *11*, 3035-3048.
(52) Castelli, D. D.; Boffa, C.; Giustetto, P.; Terreno, E.; Aime, S. Design and testing of paramagnetic liposome-based CEST agents for MRI visualization of payload release on pH-induced and ultrasound stimulation. *J Biol Inorg Chem* **2014**, *19* (2), 207-214.
(53) Garello, F.; Terreno, E. Sonosensitive MRI Nanosystems as Cancer Theranostics: A Recent Update. *Front Chem* **2018**, *6*. DOI: ARTN 157 10.3389/fchem.2018.00157.

(54) Aime, S.; Fedeli, F.; Sanino, A.; Terreno, E. A R-2/R-1 ratiometric procedure for a concentration-independent, pH-responsive, Gd(III)-based MRI agent. *J Am Chem Soc* **2006**, *128* (35), 11326-11327.